COMPUTATIONAL MODELS FOR PREDICTING THE DEFLECTED SHAPE OF A NON-UNIFORM, FLEXIBLE FINGER

Xuecheng Yin, Kok-Meng Lee, and Chao-Chieh Lan
The George W. Woodruff School of Mechanical Engineering
Georgia Institute of Technology
Atlanta, GA 30332 –0405
gt8442b@prism.gatech.edu; kokmeng.lee@me.gatech.edu; gtg032j@mail.gatech.edu

Abstract—Motivated by the applications of flexible fingers (capable of offering large deflections to accommodate object variations) in grasping, we present several computational models that characterize the large deflection of a flexible finger (beam). Specifically, we develop analytical methods for analyzing the design of cantilever-like fingers or elements of a machine that is designed primarily to support forces acting perpendicular to the axis of the member. Both uniform and non-uniform beams are considered. The methods were numerically validated by comparing the computed results against those obtained using the closed-form solutions, where exact solutions are available for fingers with a uniform cross-section. To extend the closed-form solution for predicting the shape of a non-uniform finger, we compute numerically an effective *EI* that approximates the non-uniform finger as a uniform finger at the point of contact. The approximate model has been examined experimentally. The results show excellent agreement. We expect that the methods presented here will have other engineering applications.

Index terms— grasping, flexible fingers, beam theory, handling

I. INTRODUCTION

Traditionally, designers of mechanical components are used to the assumption of rigid bodies and rigid joints. As a result, elastic deformation is often seen as something that would lower the performance of a machine. However, many real life examples demonstrate that flexible-beam-like compliance can be an advantage in many applications.

Beam theory has played an important role in the development of flexible fingers, flexural joints, compliant mechanisms, μ-motion manipulator, and nano-positioning-stages. Most of these devices have been designed upon the concept of the English clockmaker John Harrison (1759), who replaced the revolute joints with flexural pivots to remove joint friction for his chronometer. Another good application of cantilevers is its use in the atomic force microscope (AFM) [Tortonese, 1991; Baselt, 1993; Minne *et al.*, 1998; Harley [2000]. Recently, cantilevers are widely used in the Micro-Electro-Mechanical System (MEMS) technology, which takes advantage of the state-of-art integrated circuit (IC) fabrication techniques from the semiconductor industry. Some of these examples include the electrostatic-MEM switch [De Los Santos, 1997], the μ-mirror/μ-laser arrays proposed by Cheng *et al.* [1997] for replacing conventional laser printing mechanisms to print faster and eliminate synchronization problems that improve image quality while lower production costs, and the micro-machined resonant magnetic field sensor [Thierry *et al.*, 2001]. More recently, μ-cantilevers have also found their uses in fast growing bio-medical research. Wu *et al.*

[2001] developed a cantilevered microscopic chip, no bigger than a hair and coated with antibodies, for detecting prostate specific antigen (PSA) in human blood. The cantilevered chip bends like a diving board as PSA sticks to the antibodies, but does not bend when it exposes to different proteins found in human blood serum (human plasminogen (HP) and human serum albumin (HSA) because these molecules do not bind to the antibody to PSA. Most of these studies, however, were based on a linearized form of the beam equation (or the Euler-Bernoulli equation) to simplify analyses and thus, are limited to small-deflection applications.

Flexible fingers have also been widely used in poultry industry. Primary applications of flexible fingers (or beams) are for removing feathers from bird carcasses, for singulating birds into a single file to facilitate electronic counting and transportation from farms to the processing plants, and more recently for high-speed repetitive grasping of live objects [Lee, 2000], where impacts on objects are intolerable. Flexible beam undergoing large deflections also finds its usage in sports field for vaulting simulation [Ganslen, 1979; Linthorne, 2000], where the flexible pole acts as an energy transformer that converts the kinetic energy of the vaulter into the potential energy in the vaulting process. The advantages of flexible fingers are under-exploited (particularly for grasping), however, because their design involves complicated analysis.

The geometrical solution to the 2nd order, nonlinear differential equation that characterizes the large deflection of flexible beams can be found in [Frisch-Fay, 1962] but the derivation of this closed-form solution is rather cumbersome and is valid for beams with a uniform cross-section. Numerical methods, such as finite element (FE) method, are capable of solving more general problems [Yang, 1973]. An alternative solution approach is to replace the flexible beam by two rigid links connected by a "characteristic pivot" with a torsion-spring. Howell and Midha [1995] used this pseudo-rigid-body (PRB) model to analyze compliant mechanisms with small-length flexural pivots. Since the effective stiffness of the flexible beam is dependent on the location at which the force acts, the PRB model is limited to analyses where a known force applies at a specified point. To explore the use of flexible fingers for grasping live objects, Lee [1999] [Lee *et al.* 2001] extended the solution of Frisch-Fay [1962] to predict the contact point between a flexible finger and an ellipsoid. However, most of the techniques available to date are limited to beams with a uniform cross-section.

We present here three computational methods for predicting the deflected shape of a general finger with a non-uniform flexural rigidity to allow for broader applications. The remainder of this paper is organized as follows: In Section II, models for predicting the shape of a deflected finger are

0-7803-8232-3/04/$17.00 ©2004 IEEE   **2963**

presented. The models are compared in Section III. Section IV offers a method to compute an effective EI, which provides a means to extend the closed-form solution for solving the shape of a non-uniform finger. Conclusions are given in Section V.

II. FLEXIBLE BEAM MODEL

Consider a beam (which has a small y and z dimensions as compared to the x dimension) with one end clamped as shown in Figure 1, where the force F acts at an angle α at C (x_c, y_c); $Q(x, y)$ is an arbitrary point on the deflected finger; s and L are the arc lengths from the finger base to $Q(x, y)$ and C (x_c, y_c) respectively; and ψ_o is the slope of the finger at the contact.
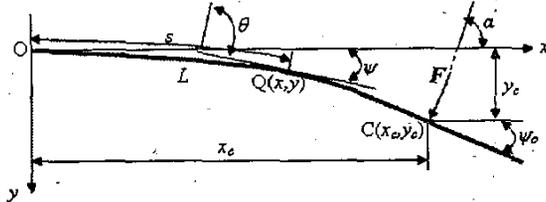

Figure 1 Schematics illustrating the parameters of the beam

The bending moment M at $Q(x, y)$ can be shown to be

$$M = EI(s)\frac{d\psi}{ds} = F\sin\alpha(x_c - x) + F\cos\alpha(y_c - y) \qquad (1)$$

where ψ is the angular deflection; E is the Young's module of the material; I is the 2nd order moment of area of the beam. Equation (1) can be written as [Yin, 2003]

$$I(u)\frac{1}{L^2}\frac{d^2\theta}{du^2} + \frac{dI(u)}{du}\frac{1}{L^2}\frac{d\theta}{du} + \frac{F}{E}\sin\theta = 0 \qquad (2)$$

where $\qquad u = s/L \in [0,1] \qquad (2a)$

and $\qquad \theta = \alpha + \psi \in [\alpha, \alpha + \psi_0] \qquad (2b)$

To solve for θ (hence ψ) in Equation (2), $I(u)$ must be in closed form (or by means of a lookup table), and that the 1st-order derivative of $I(u)$ exists and is a continuous function of u.

II.1 Small Deflection of a Uniform Beam

The curvature at the point considered is given by

$$\frac{d\psi}{ds} = \frac{-(d^2y/dx^2)}{\left[1 + (dy/dx)^2\right]^{3/2}} \qquad (3)$$

For a small deflection such that $(dy/dx)^2 \ll 1$, the curvature in Equation (1) can be approximated by the 2nd derivative of y. This assumption also implies that the 2nd term on the right-hand-side of Equation (1) is negligible, which leads to

$$EI(x)\frac{d^2y}{dx^2} = F\sin\alpha(L-x), \qquad y(x=0) = y'(x=0) = 0$$

For a uniform beam, the solution to the above classical, linear moment-curvature equation is given by

$$y = \frac{FL^3\sin\alpha}{2EI}\cdot\left(\frac{x}{L}\right)^2\left(1 - \frac{x}{3L}\right) \qquad (4)$$

II.2 Large Deflection of a Uniform Beam

Equation (4) is not valid for large-deflection applications. For a beam with a uniform cross-section, Equation (2) reduces to a form of Newton's equation:

$$\frac{d^2\theta}{du^2} + (kL)^2\sin\theta = 0 \qquad (5)$$

$$\theta(u=0) = \alpha \quad \text{and} \quad \theta'(u=1) = [d\theta/du]_{u=1} = 0$$

where $\qquad k = \sqrt{\dfrac{|f|}{EI}} \qquad (6)$

where EI is known as the flexural rigidity. The closed-form solution for Equation (5) and its boundary conditions has been derived by Frisch-Fay [1962] as follows:

$$x = \frac{1}{k}[2p\sin\alpha(\cos\zeta - \cos\xi) - h(\psi)\cos\alpha] \qquad (7a)$$

$$y = \frac{1}{k}[2p\cos\alpha(\cos\zeta - \cos\xi) + h(\psi)\sin\alpha] \qquad (7b)$$

where $\qquad p = \sin[(\psi_o + \alpha)/2]; \qquad (8a)$

$$\varsigma = \sin^{-1}\left[\frac{\sin(\alpha/2)}{p}\right]; \qquad (8b)$$

$$\xi = \sin^{-1}\left[\frac{\sin[(\psi+\alpha)/2]}{p}\right]; \qquad (8c)$$

$$h(\psi) = [F(p,\xi) - F(p,\varsigma) - 2E(p,\xi) + 2E(p,\varsigma)] \qquad (8d)$$

and where $F(p,\varsigma)$ and $E(p,\varsigma)$ are the Legendre's standard form of the first and second kinds respectively. The modulus p, which governs the deflected shape of the finger, is related to the property of the finger by

$$kL = [F(p,\pi/2) - F(p,\varsigma)] \qquad (9)$$

The deflected shape of the finger under a known point force (F, α) can be computed as follows:
1. Calculate k from Equation (6) for a given flexural rigidity.
2. Solve for the module p from Equation (9) implicitly:

$$g(p) = [F(p,\pi/2) - F(p,\varsigma)] - kL = 0, \text{ where } 0 < p < 1$$

3. Calculate ψ_0 from Equation (8a), and then ς and $\xi(\psi = \psi_0)$ from Equations (8b) and (8c) respectively.
4. The deflected shape of the finger can then be obtained from Equations (7a) and (7b) respectively.

II.3 General Solution to the Flexible Beam Model

Since a closed-form solution for the general Equation (1) is not available, Equation (2) that governs the shape of the deflected finger is solved numerically. For this purpose, we rewrite Equation (2) in a standard form:

$$\theta'' = f(u, \theta, \theta'), \qquad 0 \le u \le 1 \qquad (10)$$

$$\theta(0) = \alpha, \text{ and } \theta'(1) = 0$$

where $\qquad f(u,\theta,\theta') = -L\dfrac{I'(uL)}{I(uL)}\theta' - \dfrac{FL^2}{EI(uL)}\sin\theta$

Once the solution of Equation (2) that is essentially a standard boundary value problem (BVP) is obtained, the finger shape can be computed from the following pair of equations:

$$\begin{bmatrix} x(u_0) \\ y(u_0) \end{bmatrix} = L\int_0^{u_0}\begin{bmatrix} \cos\psi \\ \sin\psi \end{bmatrix}du \qquad (11)$$

where u_0 is any value between 0 and 1. Three numerical methods, the Shooting, the finite-difference (FD), and the finite-element (FE) are discussed as follows.

Shooting Method

Equation (10) is solved numerically using the Shooting method [Burden, 1997]. The basic idea of the Shooting method is to treat the BVP as an initial value problem:

2964

$$\theta_0'' = f(u, \theta_0, \theta_0') \qquad (12)$$
$$\theta(0) = \alpha, \text{ and } \theta_0'(0) = \varepsilon$$

where ε is a guessed slope at one end of the boundary. The guessed value of ε can be adjusted by using the difference $m(\varepsilon) = \theta_0'(1, \varepsilon) - \theta_0(1)$. The recursive algorithm is to find the correct value ε with $m(\varepsilon) = 0$ as follows:

Step 1: Use $\theta_0(0) = \alpha, \theta_0'(0) = \varepsilon(1)$ to calculate $m(1)$.

Step 2: Use $\theta_0(0) = \alpha, \theta_0'(0) = \varepsilon(2)$ to calculate $m(2)$.

Step 3: Use the secant method to obtain the new estimate:

$$\varepsilon(i) = \varepsilon(i-1) - \frac{\varepsilon(i-1) - \varepsilon(i-2)}{m(i-1) - m(i-2)} m(i-1) \text{ where } i=3, 4, \dots$$

Step 4: Iterate until $|\varepsilon(i) - \varepsilon(i-1)| \le tol$, where tol is the numerical tolerance (or a small positive value governing the accuracy of the numerical calculation).

As shown in the above steps, the Shooting method requires two initial guesses of the derivatives at one end to iteratively estimate the boundary condition at the other end.

Finite Difference Model

The continuous domain $u \in [0,1]$ is discretized into $(N+1)$ equal intervals with endpoints at $u_i = ih$ (where $i=0,1,\dots, N+1$); each has a length $h = 1/(N+1)$. The derivatives in Equation (10) are then approximated by the central finite difference formula, where the exact solution is assumed to have a bounded 4th derivative to allow for replacing $\theta''(x_i)$ and $\theta'(x_i)$:

$$\theta''(u_i) = \frac{1}{h^2}[\Delta w_{i+1} - \Delta w_i] - \frac{h^2}{12}\theta^{(4)}(\xi_i) \qquad (13a)$$

$$\theta'(u_i) = \frac{1}{2h}[\Delta w_{i+1} + \Delta w_i] - \frac{h^2}{6}\theta^{(3)}(\eta_i) \qquad (13b)$$

where $w_i = \theta(u_i)$, $\Delta w_i = w_i - w_{i-1}$. Substituting the above central difference approximations into Equation (10), the following set of $N \times N$ finite-difference equations is obtained:

$$G(W) = [G_1(W) \cdots G_i(W) \cdots G_N(W)]^T = 0 \qquad (14)$$

where
$$W = [w_1 \quad w_2 \quad \cdots \quad w_{N-1} \quad w_N]^T$$

$$G_i(W) = -\Delta w_{i-1} + \Delta w_i + h^2 f\left(u_i, w_i, \frac{\Delta w_{i-1} + \Delta w_i}{2h}\right)$$

where $i = 1, 2, \dots, N$; and the boundary conditions are

$$w_0 = \alpha \text{ and } w_{N+1} = \frac{1}{3}(4w_N - w_{N-1})$$

Newton's method can be used to generate a sequence of iterations $\{(w_1^{(k)}, \dots, w_i^{(k)}, \dots, w_N^{(k)})^T\}$ converging to the solution of Equation (14). Newton's method solves for $v_1, v_2, \dots, v_N$ in each of the iterations from the $N \times N$ linear system:

$$J(w_1, \dots, w_N)(v_1, \dots, v_N)^T = -G(W) \qquad (15)$$

where J is a tri-diagonal Jacobian matrix with the ij^{th} entry for the first $(N-1)$ rows:

$$J_{i,j} = \begin{cases} -1 + \frac{h}{2}f_{y'}\left(u_i, w_i, \frac{\Delta w_{i+1} + \Delta w_i}{2h}\right), & i = j-1 \text{ and } j = 2,\dots, N \\ 2 + h^2 f_y\left(u_i, w_i, \frac{\Delta w_{i+1} + \Delta w_i}{2h}\right), & i = j \text{ and } j = 1,\dots, N-1 \\ -1 - \frac{h}{2}f_{y'}\left(u_i, w_i, \frac{\Delta w_{i+1} + \Delta w_i}{2h}\right), & i = j+1 \text{ and } j = 1,\dots, N-2 \end{cases}$$

and for the Nth row: $J_{N,N-1} = -\frac{2}{3} - \frac{2}{3}hf_{y'}\left(u_N, w_N, \frac{2}{3h}\Delta w_N\right)$

$$J_{N,N} = \frac{2}{3} + h^2 f_y\left(u_N, w_N, \frac{2\Delta w_N}{3h}\right) + \frac{2}{3}hf_{y'}\left(u_N, w_N, \frac{2\Delta w_N}{3h}\right)$$

In each of the iterations, the approximation is updated with

$$w_i^{(k)} = w_i^{k-1} + v_i \qquad (16)$$

Since J is tri-diagonal, Crout factorization algorithm [Burden, 1997] can be applied. The convergence is possible provided that the following conditions are matched:

1. The initial guess $[w_1^{(0)}, w_2^{(0)}, \dots, w_N^{(0)}]^T$ is sufficiently close to the solution.
2. The Jacobian matrix $J(w_1, \cdots, w_i, \dots, w_N)$ is nonsingular.

Finite Element Method

To construct an approximate solution by a finite-element method based on the Rayleigh-Ritz formulation, we recast Equation (2) into a weighted-integral form:

$$\int_{u_A}^{u_B} w\left[I(u)\frac{1}{L^2}\frac{d^2\theta}{du^2} + \frac{dI(u)}{du}\frac{1}{L^2}\frac{d\theta}{du} + \frac{F}{E}\sin\theta\right]du = 0 \qquad (17)$$

Using the product rule of differentiation, the first term in the integral can be written as

$$\frac{wI(u)}{L^2}\left[\frac{d}{du}\left(\frac{d\theta}{du}\right)\right] = \frac{1}{L^2}\frac{d}{du}\left(wI(u)\frac{d\theta}{du}\right) - \frac{1}{L^2}\frac{d}{du}[wI(u)]$$

As a result, Equation (17) is simplified to

$$\int_{u_A}^{u_B}\left(-\frac{I(u)}{L^2}\frac{dw}{du}\frac{d\theta}{du} + w\frac{F}{E}\sin\theta\right)du + w(u_A)Q_A + w(u_B)Q_B = 0 \qquad (18)$$

where $Q_A = -\left(\frac{I(u)}{L^2}\frac{d\theta}{du}\right)_{u_A}$ and $Q_B = \left(\frac{I(u)}{L^2}\frac{d\theta}{du}\right)_{u_B}$.

Consider a beam made up of N two-node elements, each of which has a length h. The slope θ of the eth element ($e = 1, 2\dots, N$) is approximated as follows:

$$\theta \approx \sum_{j=1}^{2}\theta_j^e \psi_j(\bar{u}) \qquad (19)$$

$$\psi_1(\bar{u}) = 1 - \frac{\bar{u}}{h} \text{ and } \psi_2(\bar{u}) = \frac{\bar{u}}{h}$$

where; $\bar{u} = u - u_{e-1} \in [0, h]$ is the local coordinate; and θ_1^e and θ_2^e are the values of θ at the two end nodes. Upon substituting θ from Equation (19) and ψ_j for w into Equation (18), we obtain the following two algebraic equations for each element:

$$\sum_{i=1}^{2}K_i^e = -Q_i^e \qquad (20)$$

where $K_i^e = \int_0^h\left[-\frac{I(\bar{u})}{L^2}\frac{d\psi_i}{d\bar{u}}\left(\sum_{j=1}^{2}\theta_j^e\frac{d\psi_j}{d\bar{u}}\right) + \psi_i\frac{F}{E}\sin(\sum_{j=1}^{2}\theta_j^e\frac{d\psi_j}{d\bar{u}})\right]d\bar{u}$

To solve for the shape of the beam, we note the following:

1. The boundary conditions $Q_2^N = 0$ and $\theta_1 = \alpha$.
2. The continuity at the nodes requires that $\theta_2^e = \theta_1^{e+1} = \theta_e$.
3. The balance of the secondary variable requires that $Q_2^e + Q_1^{e+1} = 0$.

For a beam of N elements, the following system of $N+1$ nonlinear equation can be obtained from Equation (20):

$$\begin{bmatrix} K_1^1 \\ K_2^1 + K_1^2 \\ \vdots \\ K_2^{N-1} + K_1^N \\ K_2^N \end{bmatrix} = \begin{bmatrix} -Q_1^1 \\ -Q_2^1 - Q_1^2 \\ \vdots \\ -Q_2^{N-1} - Q_1^N \\ -Q_2^N \end{bmatrix} = \begin{bmatrix} -Q_1^1 \\ 0 \\ \vdots \\ 0 \\ 0 \end{bmatrix} \quad (21)$$

where $\theta_e (e = 2,...,N+1)$ and Q_1^1 are the $N+1$ unknowns to be solved. Note that the 1st equation $K_1^1 = -Q_1^1$ is independent of the other N equations that can be solved separately. Once θ_1 is obtained, Q_1^1 can then be solved from the 1st equation.

III. SIMULATION RESULTS

The objectives of the simulation are (1) to validate the numerical model and (2) to examine the effect of non-uniform cross-section on the defected shape of the finger.

Numerical Validation (Uniform Finger)

Since exact solution is only available for a uniform beam under a point load at a location, we validate the numerical models by comparing the deflected shape of a uniform beam against the published solution. The simulation parameters are listed in Table 1.

Table 1 Simulation parameters (uniform beam)

$EI = 0.08$ Nm^2	$F = 15$ N	$N = 20$
$L = 101.6$ mm (4 inches)	$\alpha = 90°$	

The predicted shape of a deflected finger under a point load has been computed using the three numerical methods (Shooting, FD and FE) discussed above. The results are compared in Figure 2 against those calculated using the small-deflection approximation or Equation (4), and the closed-form solution given by Frisch and Fay [1962] or Equations (7)-(9).
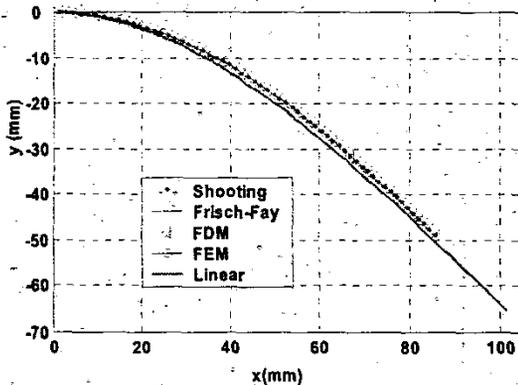

Figure 2 Numerical validations (uniform beam)

The %errors are compared in Figure 3, which is defined as

$$\%error = 100[\theta - \theta(exact)]/\theta(exact)$$

The following observations can be made from Figures 2 and 3:
1. The small deflection approximation fails to predict the shape of the finger, especially at the free end of the beam.
2. The Shooting method requires two initial guesses of $\theta'(0)$ at one end (between 0 and 1) and its accuracy depends on the scheme solving the ODE generalized in the Shooting

process; it is relatively easy to achieve higher-order accuracy. The calculated shape using the Shooting method (with 4th order Runge-Kutta or "ode45" in MATLAB) perfectly match those calculated using the Frisch-Fay solution. The algorithm converges after 6 iterations.
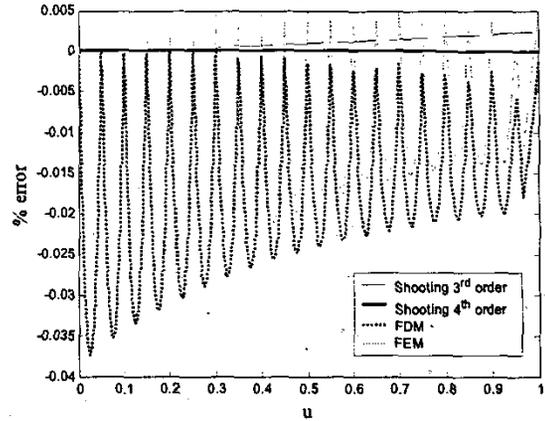

Figure 3 %Error ($N=20$ for both FD and FE methods)

3) The FD and FE methods (often referred to as a global method) interpolate between nodes, but are difficult to have higher than 2nd order accuracy. However, these methods satisfy the boundary condition (BC) automatically and thus, do not need a recursive algorithm to estimate for the BC, which is the basis of the Shooting method. The accuracy of these two methods depend on the mesh number N. The errors for both the FD and FE methods are less than 0.05% when $N=20$ as shown in Figure 3.

4) The use of Rayleigh-Ritz formulation in FE method results in Equation (20) containing terms:

$$K_i^e = -\frac{EI(\theta_e - \theta_{e+1})}{L^2 h_e} - \frac{Fh_e^2 L^2 (\sin\theta_{e+1} + \theta_e \cos\theta_e - \theta_{e+1}\cos\theta_{e-1+i} - \sin\theta_e)}{L^2 h_e E(\theta_e - \theta_{e+1})^2}$$

where $i=1,2$. The factor $(\theta_e - \theta_{e+1})^2$ in the denominator makes it ill-conditioned with a large N as u approaches 1 (i.e. the free end of the cantilever). As illustrated in Figure 4 where %error is computed at $N=100$, the error in the FE solution is less than 0.002% for $0 \le u \le 0.8$, and increases monotonically to 0.01% at the end of the cantilever.
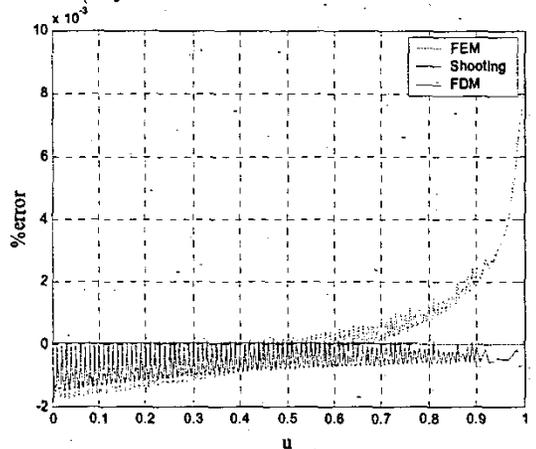

Figure 4 %Error ($N=100$ for both FD and FE methods)

Non-uniform Finger

We consider here a finger (E=4.8MPa) made up of three different cross-sections. The first part is a cone of 13mm long to provide a relatively rigid base, which is followed by the tapering 2nd part over a length of 101.76mm (4 inches). The last part is elliptical. The exponential function that approximates $I(x)$ of the beam as given as follows:

$$I(x) = Ae^{\alpha x} + Be^{\beta x} + C \tag{22}$$

where $A = 7.3 \times 10^{-8}$; $B=-3.6551 \times 10^{-8}$; $C=3.2102 \times 10^{-9}$; $\alpha=-0.07087$; and $\beta=-0.14173$. In Equation (22), x is in m; and I is in m^4. The three numerical methods were used to solve for θ subject to a normal force F=15N at L=76.2mm (3 inches).

Figure 5 shows the computed θ and the deflected finger shape calculated from Equation (11). Figure 6 compares the deflected shape of the non-uniform finger (using the Shooting, the FD, and the FE methods) against that of a uniform finger of EI=0.08Nm^2. The latter has the same slope ψ_0, at which the force exerts. As shown in Figure 6, the non-uniform finger offers the same deflection as the uniform finger at the contact point without sacrificing the rigidity near the base.
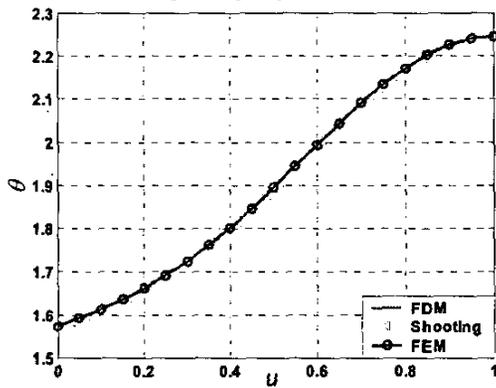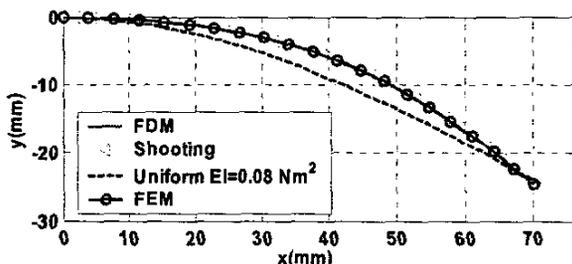

Figure 5 Comparison of computed θ

Figure 6 Finger deflection

IV. APPROXIMATION AND EXPERIMENTAL VALIDATION

For dynamic analysis and real-time control of a multiple-finger grasper, it is desired that the deflected shape of a non-uniform beam can be computed from a closed-form solution. For this reason, attempts were made to find an appropriate effective (flexural rigidity) EI such that the closed-form solution of Frisch and Fay [1962] can be applied.

Calculation of an Effective EI

The steps for finding an effective EI of a non-uniform beam under the loading (F, α; L) are given as follows:

Step 1: Calculate ψ_o (the slope of the finger at the contact point) from Equation (2b), where θ is solved numerically.
Step 2: Calculate p from Equation (8a).
Step 3: Calculate k from Equation (9).
Step 4: From Equation (6) calculate the effective EI, (EI_{eff}).
Step 5: The effective EI is given by

$$EI_{eff} = C_{EI}(EI) \tag{23}$$

where C_{EI} a correction factor. In general, the EI_{eff} (computed from Step 4) is a function of L, α and F.

As an illustration, we consider the same finger characterized by Equation (22). Figure 7 shows the effective EI calculated (from Step 4 of the above computational procedure) using the Shooting method for the flexible finger, E=4.8MPa and $I(x)$ given in Equation (22). Recall that the Shooting method requires two initial guesses of $\theta'(0)$. When $F < 30$N and $L < 0.2032$m, $\theta'(1)$ falls between 0 and 1; hence the two initial guesses were chosen between 0 and 1. When F > 30N, the range of the initial guesses is extend to 0 and 2. The computed EI is given in Table 2, where a 2nd order least square method was used to determine the correction factor.
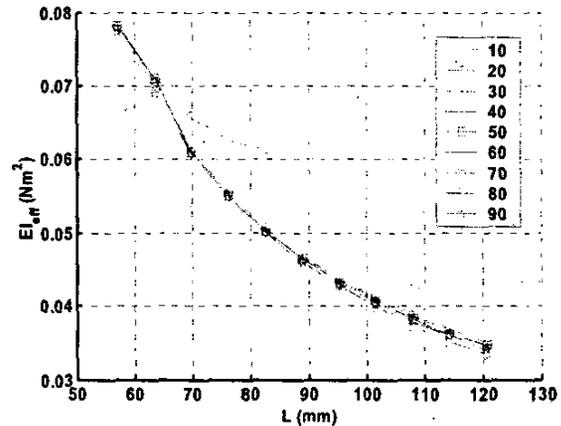

Figure 7 Computed EI as a function of L and α (F=5N)

Table 2: Example Effective EI

0.07m $< L < 0.11$m and $50^\circ < \alpha < 90^\circ$

For 2.5N $< F < 7.5$N,
$\quad C_{EI} = 1.2618 - 3.6425\,L + 34.589L^2 + 0.18541\alpha - 0.036961\alpha^2$
For 7.5N $< F < 12.5$N
$\quad C_{EI} = 1.6305 - 18.275L + 151.43L^2 + 0.32098\alpha - 0.083774\alpha^2$
For 12.5N $< F < 17.5$N
$\quad C_{EI} = 1.9609 - 28.833\,L + 254.66L^2 + 0.27266\alpha - 0.090988\alpha^2$
For 17.5N $< F < 22.5$N
$\quad C_{EI} = 1.8934 - 27.123\,L + 287.33L^2 + 0.10354\alpha - 0.069778\alpha^2$
where L is in meters; and α is in radians.

Experimental Results

To illustrate the methods for determining an effective EI that would extend the closed-form solution given by Frisch and Fay [1962] to a non-uniform beam, we evaluate the analytical prediction experimentally as shown in Figure 8, where a known force f is applied perpendicular to the x-axis (i.e., $\alpha = \pi / 2$) at a known location on the finger. Two fingers (manufactured by the Waukesha Rubber Company) with identical geometry but different materials were used, which has three non-uniform

2967

cross-sections along its length; a circular base, a taper, an elliptical section to provide rigidity in the z-direction and flexibility in the x-y plane. The Young module of the fingers were determined experimentally (Model 650M by DDL, Inc.) Other property of the finger is given in Table 3. Figure 9 compares results of two loading conditions between the predictions and the measured data, where two predictions were made; the Shooting method with an approximate geometry characterized by Equation (22), and the solution by Frisch and Fay [1962] with an effective EI given in Table 2.

Table 3: Finger properties

Parameters	Values
Mass	0.079 kg
Density	1023.43 kg/m^3
Major radius, a	12 mm
Minor radius, b	8.45 mm

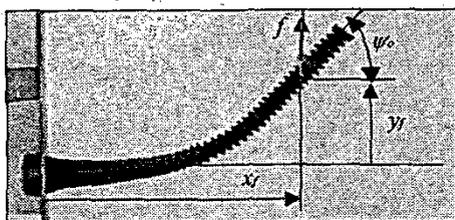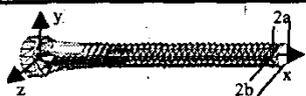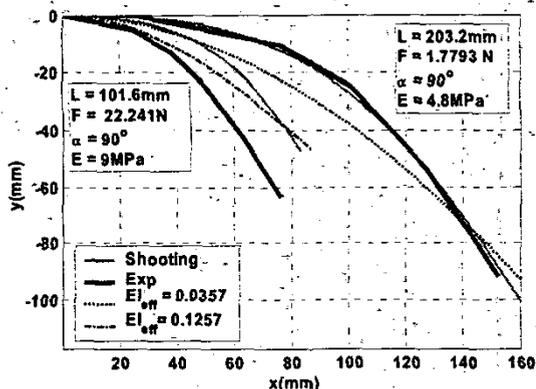E_{soft}=4.8MPa; E_{hard}=9MPa

Figure 8 Loading condition

Figure 9 Comparisons against experimental data

As compared in Figure 9, the numerical solution offers a very good prediction when the load is small and acts at a location far from the base. Closed-form solution with an effective EI provides a reasonable approximation of the numerical solution around the contact point. The discrepancy between the numerical prediction and the experimental shape becomes significant as the load is closer to the base, where the beam assumption (that the y and z dimensions are small as compared to the x dimension) is no longer valid.

V. CONCLUSIONS

Three computational methods and an approximate model for predicting the deflected shape of a flexible finger have been presented. Both uniform and non-uniform fingers were considered. The methods were numerically validated by comparing the computed results against those obtained using

the closed-form solutions derived by Frisch and Fay [1962] where exact solutions are available for fingers with a uniform cross-section. The results show excellent agreement. To extend the closed-form solution for predicting the shape of a non-uniform finger, we compute numerically an effective EI that approximates the non-uniform finger as a uniform finger at the point of contact. The approximate model has been examined experimentally. Results of the approximate model well match those obtained experimentally.

REFERENCES

Baselt, D. 1993, http://stm2.nrl.navy.mil/how-afm/how-afm.html.

Cheng, H-M., M. T. S. Ewe, R. Bashir, and G. C. T. Chiu, 2001, "Modeling and Control of Piezoelectric Cantilever Beam Micro-Mirror and Micro-Laser Arrays to Reduce Image Banding in Electrophotographic Processes," *J. of Micromechanics and Microengineering*, pp 487-498

De Los Santos, H. J., Y.-H. Kao; Caigoy, A.L.; Ditmars, E.D., 1997, "Microwave and Mechanical Considerations in the Design of MEM Switches for Aerospace Applications," IEEE Proc on Aerospace Conf., Vol.3, pp 235-254.

Faires, J. D. and R. L. Burden, 1997, Numerical Analysis, 6th Edition, Brooks/Cole Publishing Company.

Frisch-Fay, R., 1962, Flexible Bars, Washington, Butterworths.

Gascuel, M. P., 1993, "An Implicit Formulation for Precise Contact Modeling between Flexible Solids," ACM SIGGRAPH 93, pp.313-320.

Harley, J. A., 2000 "Advances in Piezoresistive Probes for Atomic Force Microscopy," Ph.D. Dissertation, Stanford University.

Lee, K.-M., 1999, "On the Development of a Compliant Grasping Mechanism for On-line Handling of Live Objects, Part I: Analytical Model," IEEE/ASME AIM'99, Atlanta, Sept. 19-23, pp 354-359.

Lee, K.-M., 2000 "Design Criteria for Developing an Automated Live-bird Transfer System," IEEE ICRA2000, San Francisco.

Lee, K-M., J. Joni, and X. C. Yin, 2001, "Compliant Grasping Force Modeling for Handling of Live Objects," IEEE ICRA2001, May 21-26, Seoul, Korea, pp 1059-1064.

Linthorne, N. P. 2000, "Energy Loss in the Pole Vault Take-off and the Advantage of Flexible Pole," Sports Engineering, Blackwell Science Ltd, March, pp 205-218.

Minne, S. C, G. Yaralioglu, S. R. Manalis, J. D. Adams, J. Zesch, A. Alalar, and C. F. Quate, 1998 "Automated Parallel High-speed Atomic Force Microscopy," Applied Physics Letters, Vol. 72, Number 18, May, pp2340-2342.

Leïchlé, T. C., M. von Arx, and M. G. Allen, 2001, "A Micromachined Resonant Magnetic Field Sensor", IEEE MEMS, Interlaken, Switzerland, 21-25 January.

Tortonese, M., H. Yamada, R. C. Barrett, and C. F. Quate, 1991 "Atomic Force Microscopy using a Piezoresistive Cantilever," Int. Conf. on Solid-State Sensors and Actuators, pp 448-451.

Wu, G., R. H. Datar, K. M. Hansen, T. Thundat, R. J. Cote and A. Majumdar, 2001, "Bioassay of Prostate-specific Antigen (PSA) using Microcantilevers," Nature Biotechnology, Sept., Vol. 19, No. 9, pp 856 – 860.

Yang, T. Y., 1973, "Matrix Displacement Solution to Elastic Problem of Beams and Frames," Int. J. of Solids and Structures, Vol. 9, No. 7, pp 829-842.

Yin, X., 2003, *Design and Analysis of a Compliant Grasper for Handling Live Objects*, Ph.D. Thesis, The Woodruff School of Mechanical Engineering, Georgia Institute of Technology.